



Evidence for possible role of toll-like receptor 3 mediating virus-induced progression of pituitary adenomas



Xin Zheng^{a,1}, Song Li^{a,1}, Zhenle Zang^a, Jintao Hu^a, Jiayin An^a, Xiangdong Pei^a, Feng Zhu^c, Weihua Zhang^{b,**}, Hui Yang^{a,*}

^a Multidisciplinary Center for Pituitary Adenomas of Chongqing, Department of Neurosurgery, Xinqiao Hospital, Third Military Medical University, Chongqing 400037, China

^b Department of Biology and Biochemistry, College of Natural Sciences and Mathematics, University of Houston, TX, USA

^c Innovative Drug Research Centre, University of Chongqing, China

ARTICLE INFO

Article history:

Received 30 October 2015

Received in revised form

25 January 2016

Accepted 11 February 2016

Available online 15 February 2016

Keywords:

Pituitary adenoma

Progression

Toll-like receptor 3

Viruses

ABSTRACT

Tumor-related viruses are known to be involved in initiation and progression of certain tumors. However, the relationship between virus and pituitary adenomas (PAs) remains unknown. Here, we investigated infection status of three types of viruses (HPV16, HHV6B and HSV1) and expression level of toll-like receptor 3 (TLR3) in 60 human PA samples. We also determined the role of TLR3 signaling pathway on a PA cell line (GH3). We firstly found that positive rates of HPV16 and HHV6B infection were significantly higher in invasive PA samples than in noninvasive samples ($P < 0.01$). Similarly, TLR3 mRNA and protein expression also increased in invasive PA samples ($P < 0.01$). In vitro analysis indicated that GH3 cell proliferation and survival were enhanced by TLR3 activation, which was accompanied by NF- κ B activation. Our data indicate that HPV16 and HHV6B viruses may be involved in promoting the progression of PA by activating the TLR3 signaling pathway.

© 2016 Elsevier Ireland Ltd. All rights reserved.

1. Introduction

Pituitary adenomas (PAs) are usually benign tumors that account for 10–15% of all intracranial tumors (Aflorei and Korbonits, 2014). PAs can be classified according to the type of hypersecretion of pituitary hormones. Clinically non-functioning pituitary adenomas (NFPAs) and growth hormone-secreting pituitary adenomas (GH-PAs) are most common in the PAs whose first-line therapy is surgery (Colao et al., 2011). Despite their histologically benign nature, 25–55% of PAs can infiltrate adjacent structures such as bony parts of the sella turcica, sphenoid sinus and/or cavernous sinus. These adenomas are defined as “invasive PAs” (Meij et al., 2002; Scheithauer et al., 1986; Thapar et al., 1996). Invasive PAs often present a higher Ki-67 index and are related to significant

morbidity, poor prognosis, and poor response to the different alternative therapies (Di Ieva et al., 2014). Understanding of the factors affecting tumor invasion is crucial for developing new adjuvant treatments and for prognosis of PA patients.

Viral infection plays an important role in initiation and development of certain types of tumors (Cerwenka and Lanier, 2001). In total, 15–20% of human cancers are estimated to be caused by oncogenic viruses (Butel, 2000). The first human tumor-associated virus was discovered in 1964 and was named Epstein–Barr virus (EBV); this virus was found to be involved in the tumorigenesis of Burkitt's lymphoma, Hodgkin's lymphoma and nasopharyngeal carcinoma (Poreba et al., 2011). DNA viruses (e.g., hepatitis B virus, human papillomaviruses) and RNA viruses (e.g., human T-cell lymphotropic virus 1 and hepatitis C virus) were found to be associated with tumorigenesis (Bergonzini et al., 2010). Accumulating evidence suggests that virus-induced chronic inflammation and oxidative stress could promote tumor development and that chronic inflammation was often mediated by pathogen-associated molecular patterns (Read and Douglas, 2014).

Activation of the Toll-like receptor (TLR) is one of the most common pathogen-associated molecular patterns that play important roles in tumor initiation and progression. The TLR family

* Corresponding author. Multidisciplinary center for pituitary adenomas of Chongqing, Department of Neurosurgery, Xinqiao Hospital, Third Military Medical University, 183 Xinqiao Main Street, Shapingba District, Chongqing, China.

** Corresponding author.

E-mail addresses: wzhang13@uh.edu (W. Zhang), yanghui64@hotmail.com (H. Yang).

¹ Xin Zheng and Song Li contributed equally to this work.

Table 1
Patient clinical characteristics.

Case	Age (yrs)	Sex	Knosp grade	Hormonal type	Ki-67 (LI \geq 3%) ^a	HPV16 ^b	HHV6B	HSV1
1	46	F	IV	NFPA	+	P	P	N
2	50	F	III	NFPA	+	N	N	P
3	56	F	III	NFPA	+	P	P	N
4	49	F	IV	NFPA	+	P	N	P
5	46	M	III	NFPA	+	P	N	N
6	51	M	III	NFPA	–	N	N	P
7	44	M	IV	NFPA	+	N	P	N
8	51	F	III	NFPA	–	P	N	P
9	47	M	IV	NFPA	+	P	P	N
10	43	F	III	NFPA	+	P	P	P
11	55	M	IV	NFPA	+	N	P	P
12	76	M	III	NFPA	+	N	N	N
13	53	M	IV	NFPA	+	P	P	P
14	47	M	IV	NFPA	+	P	N	P
15	56	F	IV	NFPA	–	P	N	N
16	43	M	II	NFPA	–	N	N	N
17	60	F	I	NFPA	+	N	P	N
18	46	F	II	NFPA	–	N	N	P
19	27	F	I	NFPA	+	P	N	P
20	53	M	I	NFPA	–	N	N	N
21	35	F	II	NFPA	–	P	P	P
22	66	M	I	NFPA	–	P	N	P
23	53	M	II	NFPA	–	P	P	P
24	48	F	I	NFPA	–	P	N	N
25	61	M	I	NFPA	–	N	N	N
26	51	F	I	NFPA	+	N	P	N
27	60	F	II	NFPA	–	N	N	N
28	50	F	I	NFPA	–	N	N	N
29	51	F	I	NFPA	–	N	N	N
30	63	M	I	NFPA	+	N	N	N
31	54	F	III	GH	+	N	P	P
32	70	F	III	GH	+	N	P	P
33	43	M	IV	GH	–	P	N	N
34	39	F	III	GH	+	P	P	P
35	48	M	IV	GH	+	P	N	N
36	46	F	III	GH	+	N	P	P
37	30	F	IV	GH	–	P	N	N
38	43	F	III	GH	+	P	P	P
39	51	M	IV	GH	–	P	N	N
40	46	M	III	GH	+	N	P	P
41	42	M	IV	GH	+	P	P	N
42	42	F	IV	GH	+	P	P	N
43	46	F	IV	GH	+	P	P	N
44	41	F	IV	GH	–	P	N	N
45	46	M	IV	GH	–	P	N	P
46	45	M	II	GH	–	N	N	N
47	45	M	I	GH	–	N	N	N
48	55	F	I	GH	–	P	N	N
49	34	M	I	GH	–	P	N	N
50	46	M	II	GH	–	N	P	N
51	46	M	I	GH	–	N	N	P
52	40	F	I	GH	+	P	P	N
53	44	F	II	GH	–	N	N	P
54	37	M	I	GH	–	N	N	N
55	46	M	II	GH	+	N	P	N
56	37	M	II	GH	–	N	N	P
57	51	F	II	GH	+	N	N	P
58	40	F	I	GH	–	N	N	N
59	37	M	I	GH	–	N	N	N
60	40	M	I	GH	–	N	N	N

^a “+” indicates Ki-67 LI \geq 3%; “–” indicates Ki-67 LI $<$ 3%.

^b “P” indicates positive detection of oncoviruses; “N” indicates negative detection of oncoviruses.

includes 10 members (TLR1–TLR10) in humans (Kawasaki and Kawai, 2014). TLR3, which is widely detected in human tumor cells, recognizes double-stranded RNA from viruses, mammalian RNA associated or released from necrotic cells, and synthetic ligand polyinosinic:polycytidylic acid [Poly(I:C)] (Huang et al., 2008; Amarante and Watanabe, 2010). TLR3 expression is related to dedifferentiated status, worse prognosis, lymph node invasion, recurrence and higher tumor metastasis probability (Chuang et al.,

2012; Saint-Jean et al., 2011).

In this study, we evaluated the infection status of three oncoviruses (HPV16, HSV1, and HHV6B) and analyzed the expression of TLR3 mRNA and protein in PA tissues. Furthermore, we determined whether activation of the TLR3 signaling pathway by viral mimic Poly(I:C) could affect the proliferation, apoptosis, and invasion of as well as cytokine production by a PA cell line in vitro.

Table 2
Primer list for nested PCR.

Virus type	Primer sequences (5'-3')	Tm cycles	Product (bp)
HPV16	F: AGGAGCGACCCAGAAAGTTACC	52–40	426
	R: CTCTACGTGTTCTTGATGATCTGCA		
in	F: TACTGCGACGTGAGGTATATGACTT	52–30	228
	R: CAGGACACAGTGGCTTTTGACAG		
HHV6B	F: TCCTGGGACCTCGTGCTAGACA	54–40	580
	R: GCGTAGAAGACAAATCCACAGCG		
in	F: AGGCTAATTGAAAGTCCACGGTT	50–30	279
	R: CGTTTGACGATAAAGGCATGACA		
HSV1	F: CGGACTTGGCTTTAGCGTG	52–40	546
	R: CACCGACCCGTATGAGACCA		
in	F: TCTTCGGAATGCTTTGGCGG	53–30	251
	R: TGGCATTCTGGGCGTGTGT		

Table 3
Primer list for qPCR.

Gene name (Species)	Primer sequences (5'-3')	Tm cycles	Product (bp)
TLR3 (human)	F: TGCCGTCTATTTGCCACACACT R: CAGGTGGCTGCAGTCAGCAA	58–35	209
β -actin (human)	F: GCACCACACCTTCTACAATGAGC R: TAGCACAGCCTGGATAGCAACG	58–35	163
TLR3 (rat)	F: GCAACAACAACATAGCCAAC R: CCTTCAGGAAATTAACGGGAC	57–30	138
β -actin (rat)	F: GAGGGAAATCGTGCCTGAC R: GCATCGGAACCGCTCATT	57–30	157

2. Materials and methods

2.1. Patients

In total, 60 patients with pituitary adenomas who underwent transsphenoidal surgery via a transnasal approach at Xinqiao Hospital in Chongqing, China were included in the study. The diagnoses of GH-PA and clinical NPPA were according to clinical and hormonal evaluation with additional information provided by pathological assessment. Thirty GH-PAs and thirty NPPAs were included.

Tumor invasiveness was determined based on magnetic resonance imaging using the modified Knosp's criteria combined with intraoperative findings. According to the Knosp classification system, the invasive adenomas are grades 3 and 4, referring to cavernous sinus invasion (Knosp et al., 1993). Based on these criteria, 30 patients consisting of 14 men and 16 women with an average age of 48 yrs (range, 30–76 yrs) had invasive PA (Table 1). Thirty patients consisting of 16 men and 14 women with an average age of 35 yrs (range, 27–66 yrs) had noninvasive PA (Table 1). This study was conducted with an approval from the Ethics and Clinical Research Committee of Xinqiao Hospital, and written informed consent was obtained from all patients or their legal guardians.

2.2. Cell culture

The rat pituitary adenoma cell line GH3 was obtained from American Type Culture Collection (ATCC, Manassas, VA, USA) cultured in Ham's F-12K medium (Invitrogen Life Technologies, Carlsbad, CA, USA) supplemented with 2.5% fetal bovine serum (FBS; Invitrogen Life Technologies) and 15% horse serum (HS; Invitrogen Life Technologies) in a 5% CO₂-humidified atmosphere at 37 °C.

2.3. Nested PCR

DNA was extracted from biopsy samples using a tissue DNA extraction kit (Qiagen, Hilden, Germany) according to the manufacturer's instructions. Two pairs of primers (outer and inner) corresponding to the viral genome were separately used in two amplification reactions. The amplification products were fractionated by electrophoresis in a 3% agarose gel. The primer sequences used for viral DNA detection in this study are shown in Table 2.

2.4. Reverse transcription and qPCR

Total RNA was extracted using TRIzol Reagent (Invitrogen, Carlsbad, CA, USA) and then treated with DNase I to eliminate genomic DNA contamination. Reverse transcription of 1 μ g RNA was performed using a ReverTra Ace First Strand cDNA Synthesis

Kit (Toyobo, Osaka, Japan) in a final volume of 20 μ L qPCR was performed using SYBR Premix Ex Taq II (TaKaRa, Dalian, China) and a CFX96 Real-time System (Bio-Rad Laboratories, Hercules, CA, USA). The relative expression levels were calculated using the $2^{-\Delta\Delta Ct}$ method. The primer sequences used for qPCR are given in Table 3.

2.5. Immunohistochemistry and immunofluorescence

Human PA tissues were fixed in formalin and embedded in paraffin for immunohistochemistry (IHC). Five-micrometer-thick sections were dewaxed and rehydrated, and then the endogenous peroxidase activity was blocked with 0.3% hydrogen peroxide in phosphate-buffered solution (PBS) for 30 min. Next, microwave antigen retrieval was performed in 0.01 M sodium citrate buffer (pH 6.0) for 20 min. After non-specific binding sites were blocked with 1/100 diluted bovine serum albumin (BSA) in PBS with 0.3% Triton X-100 (Biosharp) for 1 h at 37 °C, the sections were incubated with anti-HPV16 E6 (1:50; Abcam, Cambridge, UK), anti-HSV1 (1:100; Abcam, Cambridge, UK), anti-HHV6B (1:100; Abcam, Cambridge, UK), anti-TLR3 (1:200; Abcam, Cambridge, UK), and anti-MMP9 (1:150; Abcam, Cambridge, UK) primary antibodies overnight at 4 °C. After the sections were washed three times for 5 min each in PBS, they were incubated with secondary goat anti-rabbit immunoglobulin conjugated to peroxidase-labeled dextran polymer (EnVision System-HRP; Boster, Wuhan, China) for 1 h at 37 °C. Then, the sections were washed three times for 5 min each. 3,3'-Diaminobenzidine (Boster, Wuhan, China) was used to visualize the immunoreactions. Last, the sections were counterstained with hematoxylin, dehydrated, and covered with coverslips. The negative control experiments were performed with only the secondary antibody.

The cultured cells were fixed in 4% paraformaldehyde and solubilized in PBS with 0.1% Triton X-100 for 25 min at room

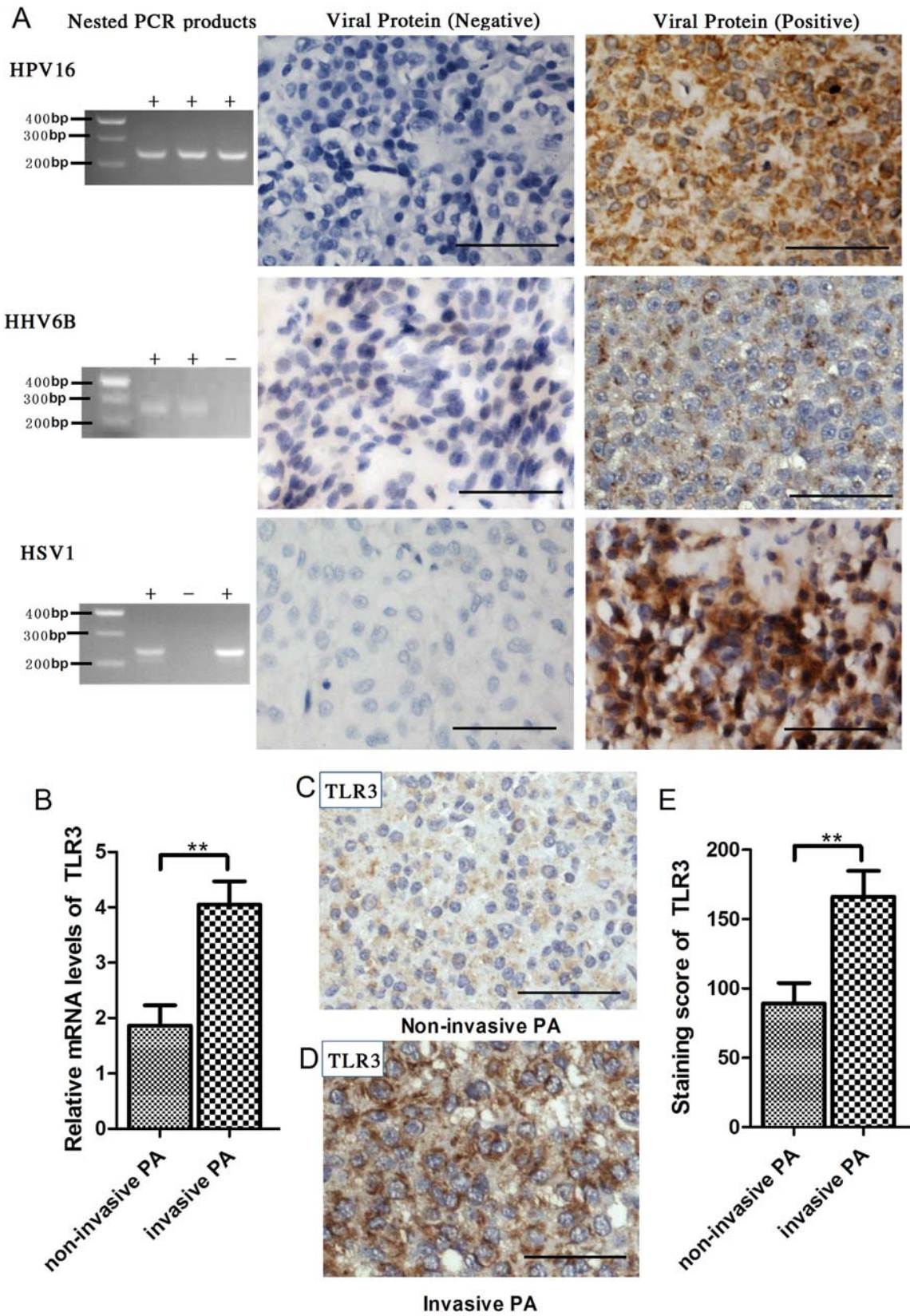


Fig. 1. Virus infections and TLR3 expression in human PA samples. A, Viral DNA was detected by nested PCR; the products are shown at their predicted band positions in the electrophoresis gel (left). “+” indicates positive DNA detection; “-” indicates negative DNA detection. Viral proteins expressed in the cytoplasm were detected by IHC (right). B, TLR3 mRNA levels in human PA samples were examined by RT-qPCR. C and D, TLR3 protein expression was detected in all 60 human PA samples by IHC. TLR3 protein was strongly expressed in the cytoplasm of invasive PA and weakly expressed in non-invasive PA. E, Staining scores for TLR3 in human PA samples. Scale bar, 50 μ m, ** $P < 0.01$.

Table 4

Detection of viral DNAs in invasive and non-invasive PA samples.

Viral DNA types	Invasive (n = 30)	Non-invasive (n = 30)	P Value
HPV16 positive (rate)	21 (70%)	8 (26.67%)	<0.01
HHV6B positive (rate)	16 (53.33%)	7 (23.33%)	<0.05

temperature on the coverslips. Non-specific binding sites were blocked for 1 h with 1/100 diluted BSA in PBS at 37 °C. The coverslips were incubated with anti-p65 (Abcam, Cambridge, UK) at 1:50 dilution overnight. After the coverslips were washed three times for 5 min each in PBS, they were stained with FITC-conjugated goat anti-rabbit IgG (1:200, Biyuntian Biotech, Jiangsu, China). Then, the coverslips were incubated with 4',6-diamidino-2-phenylindole (DAPI, 10 µg/ml, Beyotime, Nanjing, China) to counterstain the cell nuclei. After mounting the slides with anti-fading agent, a confocal laser scanning microscope (TSC-TIV; Leica, Nussloch, Germany) was used to visualize and image the fluorescent coverslips.

2.6. Western blot analysis

GH3 cell extracts equivalent to 50 µg protein were subjected to 12% SDS-PAGE and then transferred onto polyvinylidene difluoride membranes. The membranes were blocked with 5% nonfat milk in Tris-buffered saline containing 0.05% Tween 20, incubated with rabbit antibodies against rat TLR3 (1:1000; Abcam), Bcl-2 (1:1000; Abcam), Bax (1:1000; Abcam), cyclin D1 (1:500; Abcam), Caspase 3 (1:500; CST), and p65 (1:500; Abcam) and with mouse antibodies

against β-actin (1:1000; Abcam) and lamin A (1:500; Abcam). The membranes were further incubated with horseradish peroxidase-conjugated goat anti-rabbit and anti-mouse IgG (1:2000; Santa Cruz Biotechnology). The membrane signals were visualized by enhanced chemiluminescence.

2.7. Small interfering RNA (siRNA) experiments

The rat TLR3 siRNA sequences (5'-GCAAUACUUUCA-CAGGAUUDtT-3', 5'-AAUCCUGUGAAAGUAUUGCdTt-3') and scramble RNA were synthesized by Ribobio (Guangzhou, China). GH3 cells were transiently transfected with TLR3 siRNA and scramble RNA using riboFECT™ CP Reagent (Ribobio, Guangzhou, China) according to the manufacturer's instructions. Total RNA and proteins were obtained from siRNA-transfected GH3 cells. siRNA transfection efficiency was determined by real-time PCR and Western blot.

2.8. Cell proliferation assay

Cell proliferation was measured using a WST-8 Cell Counting Kit-8 (Dojindo Laboratories, Mashiki-machi, Kumamoto, Japan) according to the manufacturer's instructions.

2.9. Cell cycle analysis

Cell cycle distribution was analyzed by flow cytometry. In total, 1.0×10^6 cells were harvested at the indicated time points with relative treatment. Then, cells were rinsed with PBS, fixed in 70% ethanol at 4 °C overnight. Subsequently, the cells were resuspended

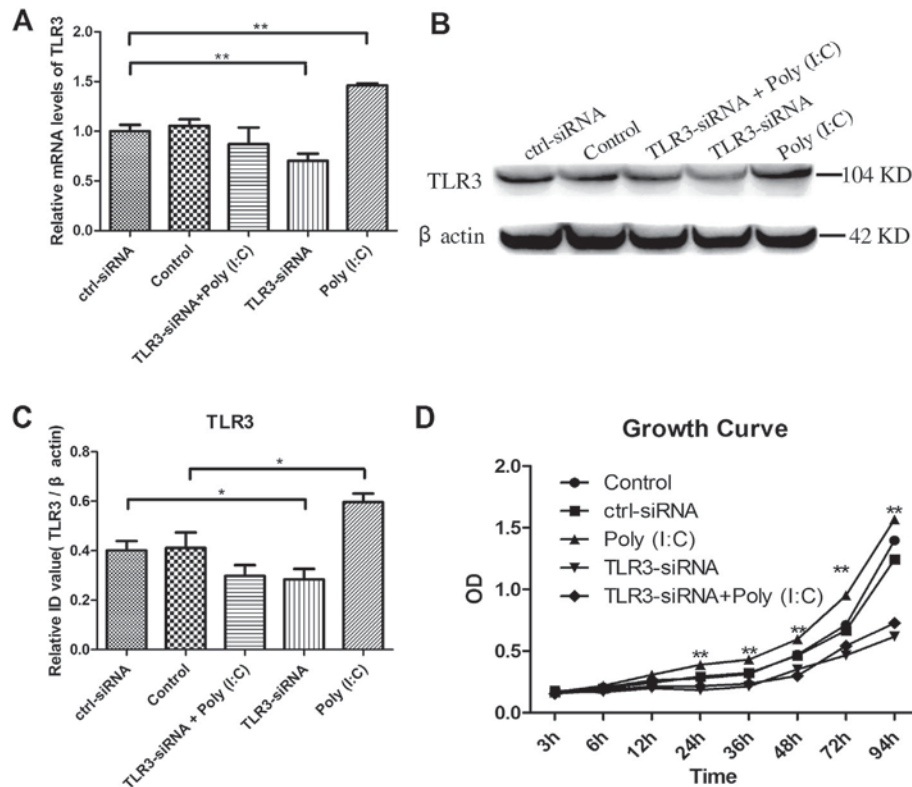
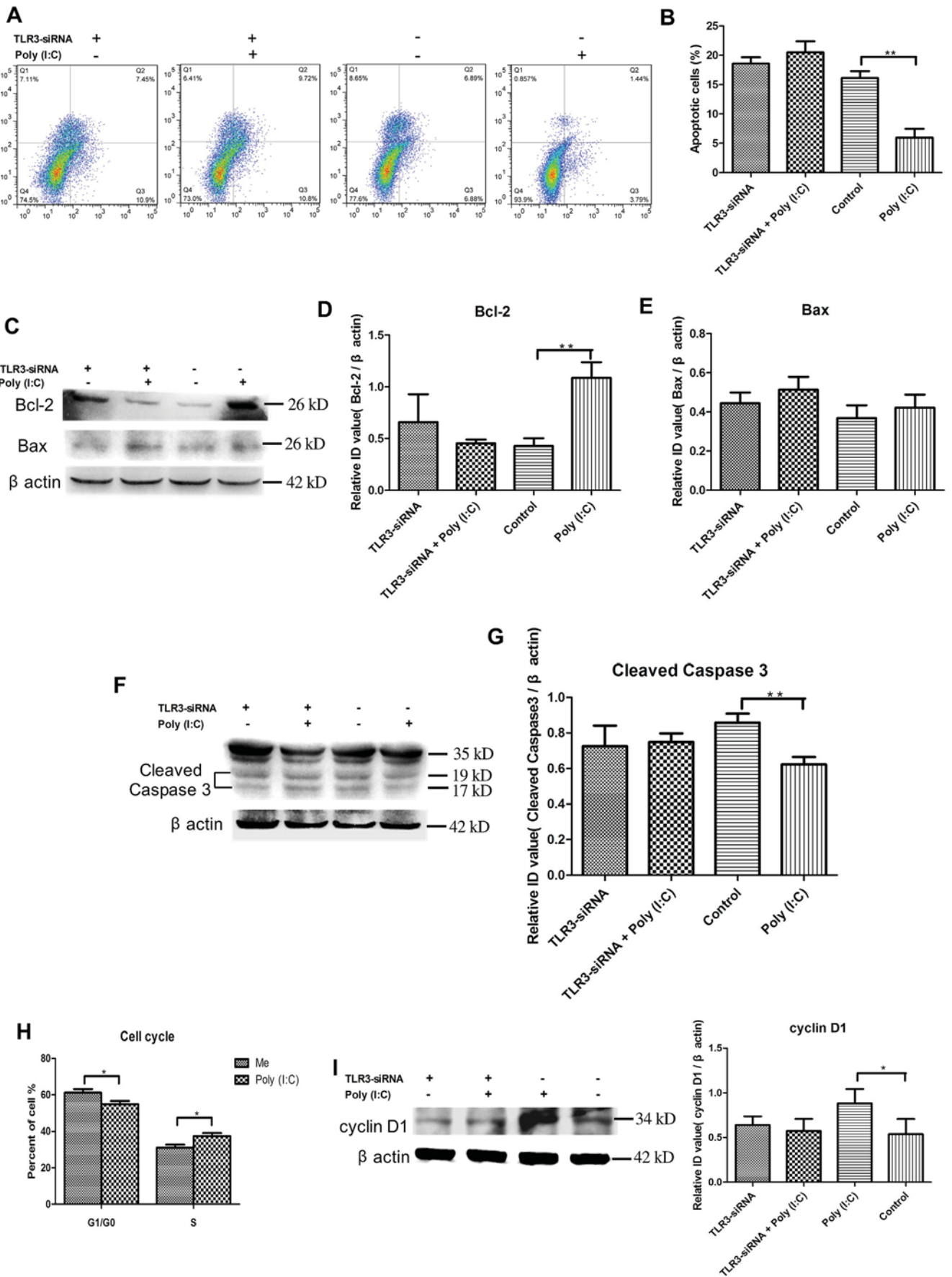


Fig. 2. TLR3 can be activated and stimulated by Poly(I:C), thus stimulating GH3 cell proliferation. A, Detection of TLR3 mRNA levels in 5 different treatment groups by RT-qPCR. B, The protein level of TLR3 was confirmed by Western blot analysis; β-actin was used as the internal control. C, The bar graph demonstrates the level of TLR3 expression compared with β-actin expression. Error bars reflect the standard error from at least 3 independent experiments. D, Cell proliferation was assessed by a CCK-8 assay. The data are expressed as the mean of three separate experiments. Eight time points were checked, and at 24 h, the difference between the Poly(I:C) treatment group and all other groups began to be significant ($P < 0.01$). * $P < 0.05$; ** $P < 0.01$.



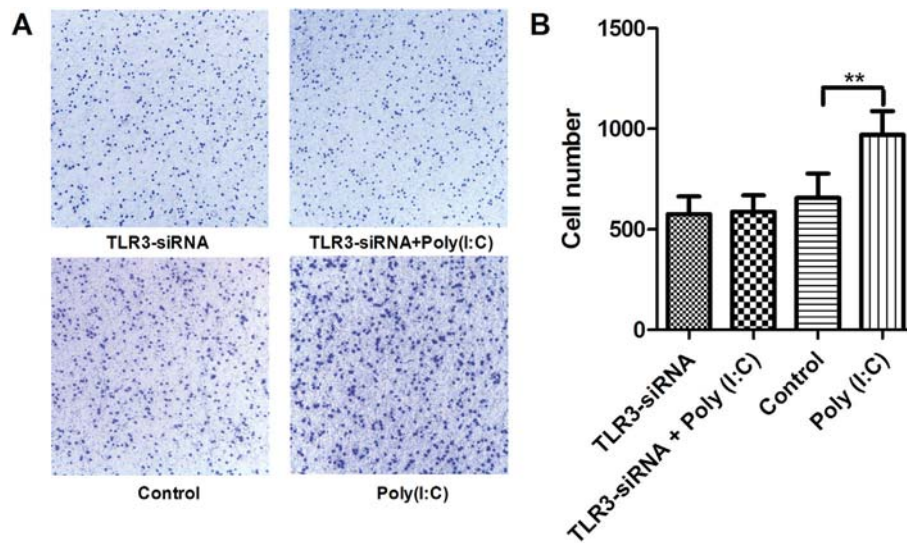


Fig. 4. GH3 cell invasion is promoted by TLR3 activation. A, Cell invasion was evaluated by Transwell assay. After different treatments, cells that penetrated through the Matrigel to the lower surface of the filter were stained by crystal violet solution and imaged. Magnification, $\times 100$. B, Statistical analysis of cell numbers in different treatment groups. ** $P < 0.01$.

and stained in 0.05 mg/ml propidium iodide (PI; BD Biosciences Pharmingen) and analyzed by flow cytometry (FACScan; BD Biosciences Pharmingen, San Diego, CA, USA). Gating was set to exclude cell debris, cell doublets, and cell clumps. DNA histograms were analyzed by ModFit LT V2.0 software.

2.10. Apoptosis analysis

GH3 cells were treated at the indicated time points with relative treatment. After treatment, apoptosis was assessed using a FITC-Annexin V apoptosis detection kit (BD Biosciences Pharmingen). Cells were washed 3 times with PBS and suspended in binding buffer. Then, the cells were stained with FITC-Annexin V and PI. Last, apoptosis was detected by flow cytometry and analyzed by ModFit LT V2.0 software.

2.11. Cell invasion assay

Invasion assay filters (8- μ m pore; Costar, Bethesda, MD, USA) were precoated with 30 μ l Matrigel (BD Biosciences, USA) for 3 h. Cells were starved for 24 h in serum-free medium, then trypsinized, resuspended in serum-free medium and placed in the precoated upper chamber of the Transwell insert (1×10^5 cells/well). Full medium containing 2.5% FBS and 15% HS was added to the lower chamber. After cells were cultured for 24 h with the indicated treatment, the nonmigrated cells in the upper chamber were mechanically removed with a cotton swab. The cells that invaded the other side of the membrane were stained with crystal violet staining solution (Boster, Wuhan, China) and then imaged. Cell numbers were counted under light microscopy at $400\times$ magnification for 5 different fields of view. (Leica, DMI3000 B).

2.12. Enzyme-linked immunosorbent assay (ELISA)

The levels of IL-6, IL-1 β , and TNF α were measured in the cell culture supernatants using ELISA kits (USCNA, Wuhan, China) at the indicated time points with relative treatment according to the manufacturer's recommendations.

2.13. Statistical analysis

The data are expressed as the mean \pm SEM. The means were compared using analysis of variance (ANOVA), and the correlations between the positive infection rates of viruses and invasiveness of PAs were determined by chi-square test. P values less than 0.05 were considered significant. These analyses were performed using SPSS for Windows version 13.0 (SPSS Inc., Chicago, IL, USA).

3. Results

3.1. Infection rates of HPV16 and HHV6B are higher in invasive PA samples

Three types of oncoviral DNAs were detected in 60 human PA sample by nested PCR (Fig. 1A). HPV16 DNA was detected in 21 (70%) invasive PA samples and in 8 (26.67%) non-invasive samples. HHV6B DNA was detected in 16 (53.33%) invasive PA samples and in 7 (23.33%) non-invasive samples. HSV1 DNA was detected in 15 (50%) invasive PA samples and in 9 (30%) non-invasive samples. The positive rate of HPV16 and HHV6B infection, but not HSV1 infection, positively correlated with the invasiveness of PA ($P < 0.05$) (Table 4). All the viral DNA-positive PA samples also expressed the corresponding viral proteins (Fig. 1A). These results indicate that HPV16 and HHV6B might be involved in the progression of invasive PA.

Fig. 3. Apoptosis and the cell cycle are affected by TLR3 activation. A, Apoptosis was measured in different treatment groups by Annexin V/propidium iodide (PI) staining. B, The histogram represents the mean from three independent experiments with standard deviation shown as error bars. C, Bcl-2 and Bax protein expression levels were examined by Western blot. For each protein, a representative blot of three experiments is shown. D and E, The bar graphs represent the mean and SEM densitometric values of three experiments. F, Cleaved caspase 3 protein expression levels were examined by Western blot. G, The bar graphs represent the mean and SEM densitometric values of three experiments. H, Cell cycle analysis by flow cytometry. Cells in the Poly(I:C)-treatment group exhibited more cells in S phase and fewer in G1 phase. I, Cyclin D1 protein expression levels were examined by Western blot; the bar graphs represent the mean and SEM densitometric values of three experiments. * $P < 0.05$; ** $P < 0.01$.

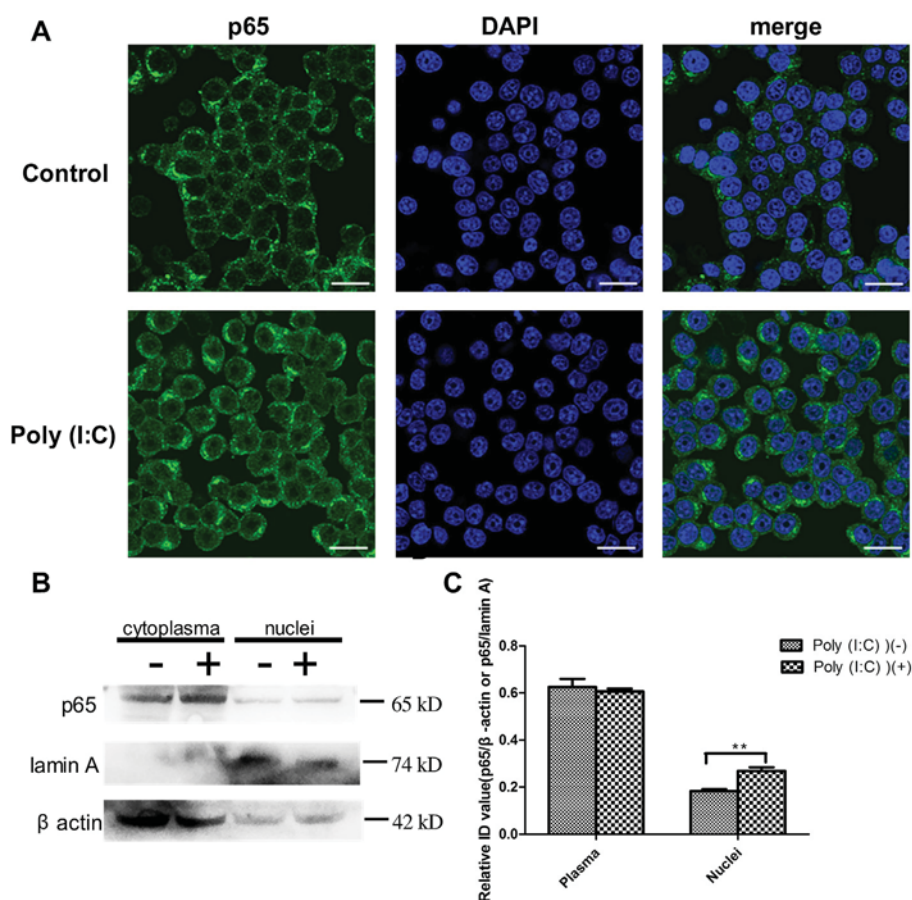


Fig. 5. Downstream NF- κ B is activated due to TLR3 activation. A, NF- κ B activation was confirmed by evaluating the subcellular localization of NF- κ B p65 through laser confocal microscopy. NF- κ B p65 (green) was weakly expressed in nuclei of control group cells but aggregated in the nuclei of Poly(I:C) treatment group cells. The nuclei were stained by DAPI (blue). B, Detection of NF- κ B p65 protein levels in the plasma and nuclei of Poly(I:C) treatment and control group cells by Western blot. Lamin A was used as the internal control for nuclear p65, and β -actin was used as the internal control for cytoplasmic p65. “-” represents the control group; “+” represents the Poly(I:C)-treated group. C, The bar graphs represent the mean and SEM densitometric values of three experiments. Scale bar, 20 μ m, ** $P < 0.01$.

3.2. TLR3 mRNA and protein expression levels are increased in invasive PA samples

During bidirectional transcription of opposing viral DNA strands, the generated dsRNA can bind and activate TLR3 independent of viral types (Thompson et al., 2011). Both TLR3 mRNA and protein were detected in PA samples. Increased TLR3 mRNA expression was observed in the invasive PA samples ($P < 0.01$, Fig. 1B). TLR3 protein was expressed in every PA sample, however quantification of cytoplasmic TLR3 levels, which were determined by semi-quantitative optical analysis as described in our previous study (Zhou et al., 2011), showed that the TLR3 level in invasive PAs was significantly higher than that in noninvasive PAs ($P < 0.01$, Fig. 1E).

3.3. TLR3 expression in the GH3 cell line can be stimulated by Poly(I:C)

Poly(I:C) is a type of synthetic analog of dsRNA and a specific TLR3 ligand. In our study, we used lower molecular weight Poly(I:C) [Poly(I:C)-LMW] at 200 μ g/ml to treat GH3 cell line for 24 h. In the pretreatment, synthetic TLR3-siRNA and control-siRNA (ctrl-siRNA) were added to the medium separately for 24 h. Then, we measured TLR3 mRNA and protein expression. We found that Poly(I:C) could increase TLR3 expression in the GH3 cell line ($P < 0.01$, Fig. 2A–C)

and that our synthetic TLR3-siRNA could inhibit TLR3 expression ($P < 0.01$, Fig. 2A–C).

3.4. TLR3 activation promotes PA cell proliferation

The Ki-67 index for each patient was evaluated by the pathology department of our hospital. A Ki-67 index greater than 3% is one of the criteria of atypical PA according to the World Health Organization (WHO) classification. In total, 22 invasive PA samples and 7 non-invasive PA samples were analyzed whose Ki-67 indexes were greater than 3% (Table 1). The Ki-67 index significantly correlated with the invasiveness of PA ($P < 0.01$). To explore the effect of Poly(I:C) (200 μ g/ml) on GH3 cell proliferation, we examined 8 time points. Growth curve analysis showed that Poly(I:C) could stimulate GH3 cell proliferation through the TLR3 signaling pathway during the analyzed time points (Fig. 2D).

3.5. Apoptosis and the cell cycle are affected by TLR3 activation

As Poly(I:C)-induced TLR3 activation could stimulate GH3 cell proliferation, we examined whether TLR3 activation could affect apoptosis and the cell cycle. We stimulated GH3 cells with 200 μ g/ml Poly(I:C) for 24 h. Before stimulation, two cell groups were treated with TLR3-siRNA for 24 h. Then, a FITC-Annexin V apoptosis detection kit and PI staining were used to examine apoptosis and

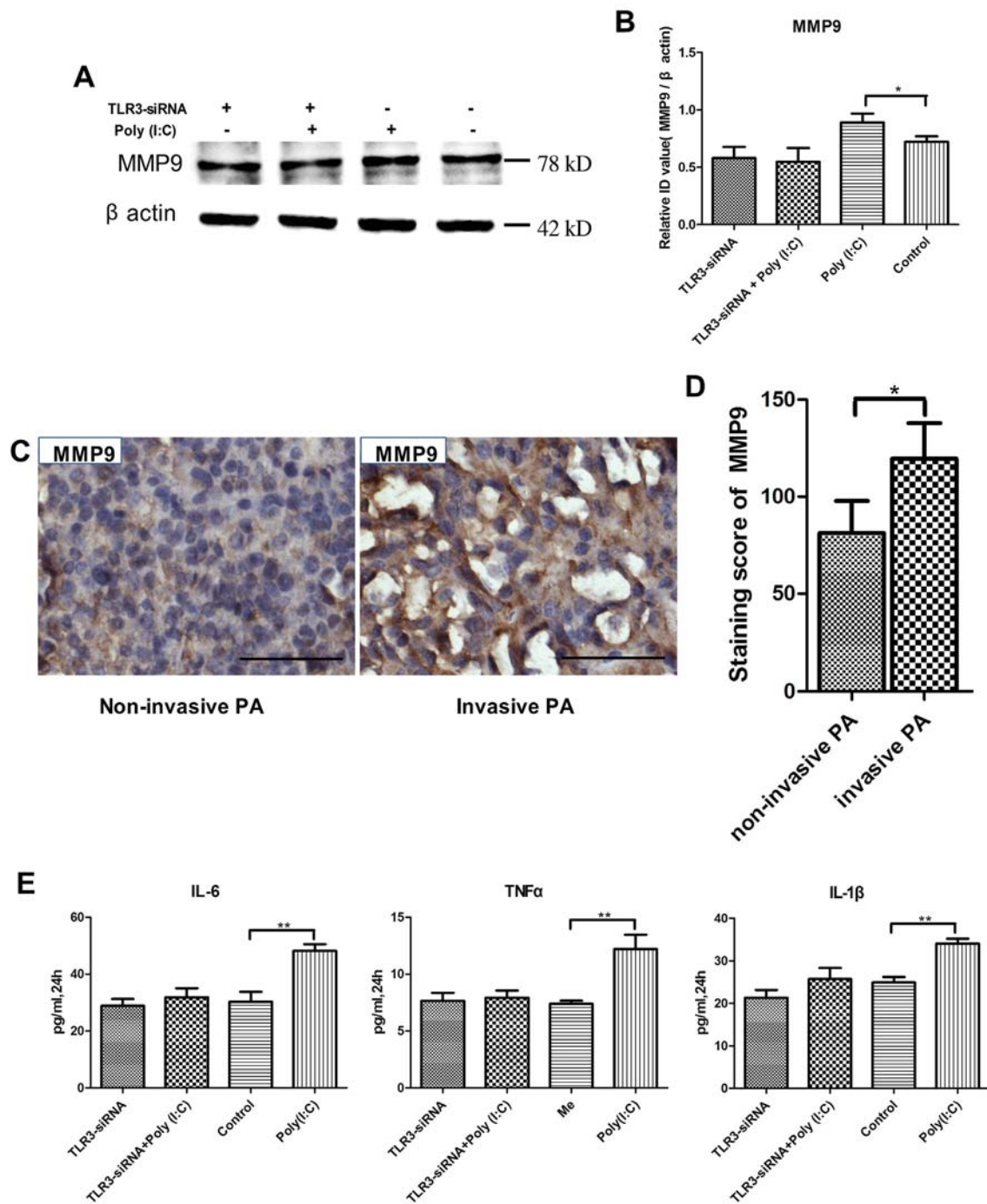


Fig. 6. Secretion and expression of cytokines and proteins related to NF- κ B activation. A, MMP9 expression in different treatment groups was evaluated by Western blot. B, The bar graphs represent the mean and SEM densitometric values of three experiments. C, Detection of MMP9 expression in human PA samples by IHC. D, Staining score statistics for MMP9 in human PA samples. E, Detection of the inflammatory cytokines IL-6, IL-1 β , and TNF α by ELISA. The results are expressed as the mean \pm SEM of 3 independent experiments. Scale bar, 50 μ m (C). * $P < 0.05$; ** $P < 0.01$.

the cell cycle by flow cytometry. We found fewer apoptotic cells (Fig. 3A, B) and more S phase cells (Fig. 3H) in the Poly(I:C)-stimulated group as compared to the control group. Then, we detected the expression of the apoptosis-related proteins, Bcl-2, Bax and Caspase 3. We found that Bcl-2, which can inhibit apoptosis, had high expression levels in the Poly(I:C)-stimulated group and that cleaved caspase 3 had low expression levels (Fig. 3C, D, F, G). The difference in Bax expression was not significant in the different groups (Fig. 3E). Simultaneously, we examined the

expression of cyclin D1, which regulates the G1/S phase transition and S phase entry. We found that cyclin D1 had a higher expression level in the Poly(I:C) group (Fig. 3I).

3.6. TLR3 activation can promote GH3 cell invasion

The positive rate of virus infection and TLR3 expression are higher in invasive PA. Therefore, we determined the effect of TLR3 activation on GH3 cell invasion. Poly(I:C) was added to the upper

chamber with cells that were untreated or treated with TLR3-siRNA. After 48 h, the invasive cells were stained and counted (Fig. 4A). Statistical analyses indicated that more Poly(I:C)-treated group cells through the Transwell chamber (Fig. 4B).

3.7. NF- κ B downstream of TLR3 is activated

NF- κ B is an important mediator in the TLR3 signaling pathway. Activation of NF- κ B induces genes that maintain cell proliferation, promote invasion, and activate inflammatory cytokines. Once NF- κ B is activated, its p65 subunit will be transmitted from the cytoplasm into nuclei. Therefore, we used immunofluorescence to determine the subcellular localization of the NF- κ B p65 subunit after Poly(I:C) stimulation. Moreover, we examined p65 protein expression levels in the plasma and nuclei. After cells were stimulated with Poly(I:C) for 24 h, more p65 was transmitted into the nuclei (Fig. 5A), and p65 protein expression was higher in nuclei than in plasma (Fig. 5B, C).

3.8. The expression levels of downstream inflammatory cytokines are higher in GH3 cells after Poly(I:C) treatment

MMP9 can be induced by NF- κ B activation. Many studies have shown that MMP9 is closely related to the invasiveness of PA; therefore, we measured MMP9 expression (Mete et al., 2012). We found that MMP9 expression was increased (Fig. 6A, B) by Poly(I:C). Consistent with the in vitro study, we also found that MMP9 protein expression was higher in invasive PA samples than noninvasive samples (Fig. 6C, D). Secretion of several inflammatory cytokines can be induced by NF- κ B activation. NF- κ B was shown to be activated in the Poly(I:C)-stimulated GH3 cell line; therefore, we detected the expression of the NF- κ B-regulated genes encoding MMP9, IL-6, IL-1 β and TNF α and found that these genes were up-regulated by Poly(I:C) (Fig. 6E).

4. Discussion

Although PAs are typical benign tumors, large number of these tumors exhibit invasive behaviors that directly lead to recurrence and low rate of total surgical resection (Colao et al., 2011). Several studies have shown that changes in chromosomes and genes (e.g., 11p/q and p53, respectively), adhesion molecules (e.g., E-cadherin), matrix metalloproteinases (e.g., MMP9, MMP2), inflammatory cytokines (e.g., IL-6, IL-17) are related to the progression of PA. However, the underlying mechanism remains largely unknown (Dileva et al., 2014; Mete et al., 2012; Gandour-Edwards et al., 1995; Kawamoto et al., 1996; Liu et al., 2005; Qiu et al., 2011a; Zhou et al., 2013a). In our study, for the first time, we've found a correlation between oncovirus infection and PA invasiveness in human samples and viral activation of TLR3/NF- κ B signaling is involved in the proliferation and invasiveness of a PA cell line.

Oncoviruses are known to be involved in the initiation and progression of several tumors (Read and Douglas, 2014). High-risk HPVs can initiate several types of human cancer. Moreover, several high-risk HPV-positive tumors show increased migratory and invasive properties (Poreba et al., 2011). HHV6 is a human B-lymphotropic virus responsible for severer outcomes among pediatric lymphoma patients (Loutfy et al., 2010). In our study, we found that HPV16 and HHV6B infections were positive and significantly related to the invasiveness of PA. This study is the first to confirm these viral infections in PA tumor cells and their correlation to PA invasiveness. Our findings appear to be distinct from a previous study by Woloschak et al. (1995), where they found HPV types 16, 18 and 33 were not amplified from human PA, which is possibly due to the ethnicities, region and detection technologies used.

During persistent viral infection, excessive inflammation can arise and is generally damaging; this inflammation is often a result of antiviral responses (Read and Douglas, 2014). TLR3 is an important participant in the antiviral process and in virus-induced carcinogenic inflammation. TLR3 is related to clearance of HPV in healthy population (Scott et al., 2015). HPV has also been demonstrated to modulate TLR expression and signaling, thus leading to persistent viral infection and carcinogenesis (Zhou et al., 2013b). Virus-encoded RNAs could induce inflammatory responses in nasopharyngeal carcinoma cells through TLR3, which primarily induced a high level of TNF α production; TNF α then recruited and activated macrophages, creating a protumorigenic microenvironment for solid tumor growth (Li et al., 2015). In lung cancer and head and neck cancer cell lines, TLR3 activation can induce tumor cell invasion and proliferation (Chuang et al., 2012; Zhan et al., 2014). In our study, we firstly found that TLR3 highly expressed in human invasive PA samples, indicating a correlation between TLR3 and PA invasiveness. Additionally, the GH3 cell line was used to detect the role of TLR3 in PA. By activating TLR3, GH3 cell proliferation was stimulated. Further detection showed up-regulation of the apoptosis-related protein Bcl-2 and down-regulation of cleaved caspase 3. Cell cycle analysis showed more cells in S phase along with up-regulation of the cell-cycle related protein cyclin D1. Simultaneously, an increase in GH3 cell invasion and up-regulation of MMP9 expression were observed. Our findings in human PA samples suggest that TLR3 might be involved in the progression of human PA.

NF- κ B is an important downstream transcription factor of TLR3 signaling, and NF- κ B signaling may be crucial in tumor progression. NF- κ B is considered as a key node that amplifies inflammatory responses that are induced by virus-encoded RNAs in nasopharyngeal carcinoma cells (Li et al., 2015). Several NF- κ B-regulated genes that encode serine proteases, adhesion molecules, MMPs, and chemokines have been shown to be essential for tumor invasion and metastasis (Coussens and Werb, 2002; Karin and Greten, 2005). In our in vitro study, NF- κ B was also activated in the TLR3 signaling pathway. Moreover, the NF- κ B-regulated genes encoded MMP9, IL-6, IL-1 β and TNF α were detected and found to be up-regulated along with TLR3 activation. Several previous studies have indicated that these factors might play exogenous roles in the aggressive biological behaviors of GH3 cells. Several studies have confirmed that MMP9 is correlated with both the invasiveness and angiogenesis of PA (Qiu et al., 2011b; Hussaini et al., 2007; Turner et al., 2000). IL-1 β has been shown to be involved in the regulation of somatotroph adenoma cell growth (Sauer et al., 1998). Moreover, exposure of MMQ pituitary adenoma cells to TNF α could induce VEGF and MMP-9 expression in vitro (Xiao et al., 2011). In pituitary adenomas, IL-6 stimulates the secretion of hormones, the proliferation of tumor cells, and the production of angiogenic factors, such as vascular endothelial growth factor-A (Renner et al., 2009). Further work is needed to determine the role of each of the cytokines in mediating virus induced PA progression. Since a rat but not a human PA cell line was used in our vitro study, there may be some interspecies differences in the mechanisms. More clinical studies are needed to illustrate mechanisms clearly.

5. Conclusion

In summary, the data presented here are the first to demonstrate that virus infections may contribute to the progression of PA by activating TLR3. The molecular mechanisms involved in this process might include regulation of apoptosis and cell cycle-related proteins and modulation of a pro-tumorigenic microenvironment by up-regulating inflammatory cytokines. Our findings will help us understand the mechanisms of PA progression.

Conflicts of interest

The authors declare that they have no conflict of interest.

Acknowledgments

This work was supported by National Natural Science Foundation of China Grant 81528014.

References

- Aflorei, E.D., Korbonits, M., 2014. Epidemiology and etiopathogenesis of pituitary adenomas. *J. Neurooncol.* 117, 379–394.
- Amarante, M.K., Watanabe, M.A.E., 2010. Toll-like receptor 3: involvement with exogenous and endogenous RNA. *Int. Rev. Immunol.* 29, 557–573.
- Bergonzini, V., Salata, C., Calistri, A., Parolin, C., Palù, G., 2010. View and review on viral oncology research. *Infect. Agent Cancer* 5, 11.
- Butel, J.S., 2000. Viral carcinogenesis: revelation of molecular mechanisms and etiology of human disease. *Carcinogenesis* 21, 405–426.
- Cerwenka, A., Lanier, L.L., 2001. Natural killer cells, viruses and cancer. *Nat. Rev. Immunol.* 1, 41–49.
- Chuang, H.C., Huang, C.C., Chien, C.Y., Chuang, J.H., 2012. Toll-like receptor 3-mediated tumor invasion in head and neck cancer. *Oral Oncol.* 48, 226–232.
- Colao, A., Grasso, L.F.S., Pivonello, R., Lombardi, G., 2011. Therapy of aggressive pituitary tumors. *Expert Opin. Pharmacother.* 12, 1561–1570.
- Coussens, L.M., Werb, Z., 2002. Inflammation and cancer. *Nature* 420, 860–867.
- Di Ieva, A., Rotondo, F., Syro, L.V., Cusimano, M.D., Kovacs, K., 2014. Aggressive pituitary adenomas-diagnosis and emerging treatments. *Nat. Rev. Endocrinol.* 10, 423–435.
- Gandour-Edwards, R., Kapadia, S.B., Janecka, I.P., Martinez, A.J., Barnes, L., 1995. Biologic markers of invasive pituitary adenomas involving the sphenoid sinus. *Mod. Pathol.* 8, 160–164.
- Huang, B., Zhao, J., Unkeless, J.C., Feng, Z.H., Xiong, H., 2008. TLR signaling by tumor and immune cells: a double-edged sword. *Oncogene* 27, 218–224.
- Hussaini, I.M., Trotter, C., Zhao, Y., Abdel-Fattah, R., Amos, S., Xiao, A., Agi, C.U., Redpath, G.T., Fang, Z., Leung, G.K.K., Lopes, M.B.S., Laws, E.R., 2007. Matrix metalloproteinase-9 is differentially expressed in nonfunctioning invasive and noninvasive pituitary adenomas and increases invasion in human pituitary adenoma cell line. *Am. J. Pathol.* 170, 356–365.
- Karin, M., Greten, F.R., 2005. NF-kappaB: linking inflammation and immunity to cancer development and progression. *Nat. Rev. Immunol.* 5, 749–759.
- Kawamoto, H., Kawamoto, K., Mizoue, T., Uozumi, T., Arita, K., Kurisu, K., 1996. Matrix metalloproteinase-9 secretion by human pituitary adenomas detected by cell immunoblot analysis. *Acta Neurochir. (Wien)* 138, 1442–1448.
- Kawasaki, T., Kawai, T., 2014. Toll-like receptor signaling pathways. *Front. Immunol.* 5, 461.
- Knosp, E., Steiner, E., Kitz, K., Matula, C., 1993. Pituitary adenomas with invasion of the cavernous sinus space: a magnetic resonance imaging classification compared with surgical findings. *Neurosurgery* 33, 610–617 discussion 617–618.
- Li, Z., Duan, Y., Cheng, S., Chen, Y., Hu, Y., Zhang, L., He, J., Liao, Q., Yang, L., Sun, L.Q., 2015. EBV-encoded RNA via TLR3 induces inflammation in nasopharyngeal carcinoma. *Oncotarget* 6, 24291–24303.
- Liu, W., Matsumoto, Y., Okada, M., Miyake, K., Kunishio, K., Kawai, N., Tamiya, T., Nagao, S., 2005. Matrix metalloproteinase 2 and 9 expression correlated with cavernous sinus invasion of pituitary adenomas. *J. Med. Invest.* 52, 151–158.
- Loutfy, S.A., Fawzy, M., El-Wakil, M., Moneer, M.M., 2010. Presence of human herpes virus 6 (HHV6) in pediatric lymphomas: impact on clinical course and association with cytomegalovirus infection. *Virology* 7, 287.
- Meij, B.P., Lopes, M.-B.S., Ellegala, D.B., Alden, T.D., Laws, E.R., 2002. The long-term significance of microscopic dural invasion in 354 patients with pituitary adenomas treated with transsphenoidal surgery. *J. Neurosurg.* 96, 195–208.
- Mete, O., Ezzat, S., Asa, S.L., 2012. Biomarkers of aggressive pituitary adenomas. *J. Mol. Endocrinol.* 49, R69–R78.
- Poreba, E., Broniarczyk, J.K., Gozdzicka-Jozefiak, A., 2011. Epigenetic mechanisms in virus-induced tumorigenesis. *Clin. Epigenetics* 2, 233–247.
- Qiu, L., He, D., Fan, X., Li, Z., Liao, C., Zhu, Y., Wang, H., 2011. The expression of interleukin (IL)-17 and IL-17 receptor and MMP-9 in human pituitary adenomas. *Pituitary* 14, 266–275.
- Qiu, L., He, D., Fan, X., Li, Z., Liao, C., Zhu, Y., Wang, H., 2011. The expression of interleukin (IL)-17 and IL-17 receptor and MMP-9 in human pituitary adenomas. *Pituitary* 14, 266–275.
- Read, S.A., Douglas, M.W., 2014. Virus induced inflammation and cancer development. *Cancer Lett.* 345, 174–181.
- Renner, U., De Santana, E.C., Gerez, J., Fröhlich, B., Haedo, M., Pereda, M.P., Onofri, C., Stalla, G.K., Arzt, E., 2009. Intrapituitary expression and regulation of the gp130 cytokine interleukin-6 and its implication in pituitary physiology and pathophysiology. *Ann. N. Y. Acad. Sci.* 1153, 89–97.
- Saint-Jean, M., Knol, A.C., Nguyen, J.M., Khammari, A., Dréno, B., 2011. TLR expression in human melanoma cells. *Eur. J. Dermatol.* 21, 899–905.
- Sauer, J., Renner, U., Hopfner, U., Lange, M., Muller, A., Strasburger, C.J., Pagotto, U., Arzt, E., Stalla, G.K., 1998. Interleukin-1 beta enhances interleukin-1 receptor antagonist content in human somatotroph adenoma cell cultures. *J. Clin. Endocrinol. Metab.* 83, 2429–2434.
- Scheithauer, B.W., Kovacs, K.T., Laws, E.R., Randall, R.V., 1986. Pathology of invasive pituitary tumors with special reference to functional classification. *J. Neurosurg.* 65, 733–744.
- Scott, M.E., Ma, Y., Farhat, S., Moscicki, A.-B., 2015. Expression of nucleic acid-sensing toll-like receptors predicts HPV16 clearance associated with an E6-directed cell-mediated response. *Int. J. Cancer* 136, 2402–2408.
- Thapar, K., Kovacs, K., Scheithauer, B.W., Stefaneanu, L., Horvath, E., Pernicone, P.J., Murray, D., Laws, E.R., 1996. Proliferative activity and invasiveness among pituitary adenomas and carcinomas: an analysis using the MIB-1 antibody. *Neurosurgery* 38, 99–106 discussion 106–107.
- Thompson, M.R., Kaminski, J.J., Kurt-Jones, E.A., Fitzgerald, K.A., 2011. Pattern recognition receptors and the innate immune response to viral infection. *Viruses* 3, 920–940.
- Turner, H.E., Nagy, Z., Esiri, M.M., Harris, A.L., Wass, J.A., 2000. Role of matrix metalloproteinase 9 in pituitary tumor behavior. *J. Clin. Endocrinol. Metab.* 85, 2931–2935.
- Woloschak, M., Yu, A., Post, K.D., 1995. Detection of polyomaviral DNA sequences in normal and adenomatous human pituitary tissues using the polymerase chain reaction. *Cancer* 76, 490–496.
- Xiao, Z., Liu, Q., Mao, F., Wu, J., Lei, T., 2011. TNF α -induced VEGF and MMP-9 expression promotes hemorrhagic transformation in pituitary adenomas. *Int. J. Mol. Sci.* 12, 4165–4179.
- Zhan, Z., Xie, X., Cao, H., Zhou, X., Zhang, X.D., Fan, H., Liu, Z., 2014. Autophagy facilitates TLR4- and TLR3-triggered migration and invasion of lung cancer cells through the promotion of TRAF6 ubiquitination. *Autophagy* 10, 257–268.
- Zhou, W., Song, Y., Xu, H., Zhou, K., Zhang, W., Chen, J., Qin, M., Yi, H., Gustafsson, J.A., Yang, H., Fan, X., 2011. In nonfunctional pituitary adenomas, estrogen receptors and slug contribute to development of invasiveness. *J. Clin. Endocrinol. Metab.* 96, E1237–E1245.
- Zhou, K., Jin, H., Luo, Y., 2013. Expression and significance of E-cadherin and β -catenins in pituitary adenoma. *Int. J. Surg. Pathol.* 21, 363–367.
- Zhou, Q., Zhu, K., Cheng, H., 2013. Toll-like receptors in human papillomavirus infection. *Arch. Immunol. Ther. Exp. Warsz.* 61, 203–215.